



## **SEISMIC REHABILITATION OF REINFORCED CONCRETE COLUMNS**

**Patrício ROCHA<sup>1</sup>, Pedro DELGADO<sup>2</sup>, Victorino RODRIGUES<sup>3</sup>, Miguel SANTOS<sup>4</sup>,  
António ARÊDE<sup>5</sup>, Nelson VILA POUCA<sup>6</sup>, Anibal COSTA<sup>7</sup> and Raimundo DELGADO<sup>8</sup>**

### **SUMMARY**

The main purpose of this paper is to present an experimental campaign of different strategies for the seismic retrofit of RC columns, comparing the obtained results with analytical methodologies, and evaluating benefits concerning their structural behaviour under the cyclic loading. The experimental campaign was conceived taking into account the typical constructions of the seventies, designed according to old codes without seismic considerations, and seeking the best structural retrofit technique to enable seismic behaviour improvement with acceptable financial resources. The setup of the RC columns experimental tests was specially designed to carry out biaxial bending with axial load, using two orthogonal and horizontal actuators and one vertical actuator (with a slide device to allow the top displacements of the column), though, at this stage, only uni-axial bending experimental results are available. The columns rehabilitation, improving the ductility or the strength characteristics, was obtained increasing the concrete ductility conditions, through efficient jacketing, or increasing the amount of longitudinal and transversal steel. The aim is, therefore, to contribute for developing and calibrating a procedure that enables the evaluation of the efficiency of the different retrofit solutions, their possibilities and fields of application. It was also an objective of this work to explore the possibility of use this retrofitting techniques on the improvement of buildings performance.

### **1. INTRODUCTION**

In order to analyze and assess different strategies for the seismic retrofit of RC columns, an experimental campaign is presently underway at the Laboratory of Earthquake and Structural Engineering (LESE) of the Faculty of Engineering of the University of Porto (FEUP).

The specimens have been chosen aiming at reproducing some columns of a RC frame studied within the ICONS project framework developed at the European Laboratory for Safety Assessment (ELSA) of the Joint Research Centre (JRC) at Ispra (Italy), where the frame experimental tests took place [Pinho, 2000] and [Varum, 2003]. In total, eight full-scale RC columns will be tested, both in the original undamaged state and after retrofit interventions according to different techniques.

---

<sup>1</sup> Polytechnic Institute - Apartado 574, 4901-908 Viana do Castelo, Portugal  
Email : [procha@estg.ipvc.pt](mailto:procha@estg.ipvc.pt)

<sup>2</sup> Polytechnic Institute - Apartado 574, 4901-908 Viana do Castelo, Portugal  
Email : [pdelgado@estg.ipvc.pt](mailto:pdelgado@estg.ipvc.pt)

<sup>3</sup> Porto University - Faculty of Engineering, Rua Dr. Roberto Frias, s/n 4200-465 Porto, Portugal  
Email : [vidigal.rodrigues@fe.up.pt](mailto:vidigal.rodrigues@fe.up.pt)

<sup>4</sup> S.T.A.P. – Reparação, consolidação e modificação de estruturas, S. A., Porto, Portugal  
Web pag : [www.stap.pt](http://www.stap.pt)

<sup>5</sup> Porto University - Faculty of Engineering, Rua Dr. Roberto Frias, s/n 4200-465 Porto, Portugal  
Email : [aarede@fe.up.pt](mailto:aarede@fe.up.pt)

<sup>6</sup> Porto University - Faculty of Engineering, Rua Dr. Roberto Frias, s/n 4200-465 Porto, Portugal  
Email : [nelsonvp@fe.up.pt](mailto:nelsonvp@fe.up.pt)

<sup>7</sup> Universidade de Aveiro, Campus Universitário de Santiago, 3810-193 Aveiro, Portugal  
Email : [acosta@civil.ua.pt](mailto:acosta@civil.ua.pt)

<sup>8</sup> Porto University - Faculty of Engineering, Rua Dr. Roberto Frias, s/n 4200-465 Porto, Portugal  
Email : [rdelgado@fe.up.pt](mailto:rdelgado@fe.up.pt)

This paper presents the results of the first set of tested specimens, before and after their retrofit with steel plates and with Carbon Fibre Reinforced Polymers (CFRP) sheets.

Four RC columns full scale models were designed to reproduce some columns of the ICONS frame. The specimens have 200 mm by 400 mm rectangular cross-section and are 1720 mm high from the top to the footing, the later with 1300 mm x 1300 mm x 500 mm and heavily reinforced to avoid any premature failure during testing.

The test setup, as illustrated in Fig. 1, is suitable to apply lateral loads using a hydraulic actuator attached to a reaction steel frame. For the horizontal load a 200 kN capacity actuator was used, whereas a constant axial load of 170 kN was applied to the column using a 700 kN capacity hydraulic jack supported on another independent steel portal frame. The specimen footing is bolted to the strong floor (600 mm thick) by means of four high resistance steel rods of 28 mm diameter. The vertical and horizontal frames are also fixed to the strong lab floor by means of high resistance steel rods of 28 mm. All these rods are duly prestressed with a hollow jack to prevent undesired displacements and/or rotations of both the footing and the frames. As also shown in Fig. 1 (right), the column specimen PA1 has six 12 mm diameter longitudinal rebars of A400 steel grade with average yield strength of 460 MPa; it is transversely reinforced with 6 mm diameter rebars, with 150 mm spacing, made of A500 steel grade with average yield strength of 750 MPa. The footing reinforcement is also shown and made with A400 steel grade. The average concrete compressive strength is 43 MPa, as obtained from tests performed on concrete cubes.

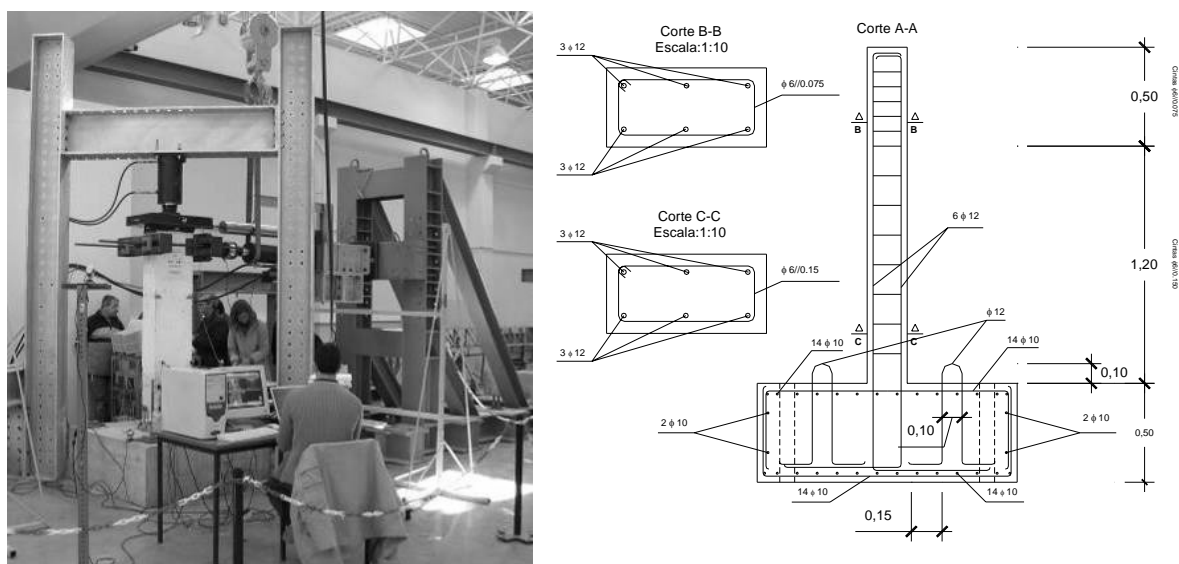


**Figure 1: View of the test setup at LESE Lab and specimen PA1.**

The specimens were named PA1-Nx, where PA1 is the model reference and x refers to the specimen number, meaning x=1, 2, 3, 4, 5 and 6.

A special device was designed to apply a constant axial load in the column, while allowing lateral displacements and top-end rotations to take place “freely”. The device consists of two steel plates with very low friction contact surfaces, where the lower plate is bonded to the specimen top-section and the upper is hinged to the vertical actuator; this plate is also connected to a stiff rod provided with a load cell to measure the residual friction force between the two plates in order to obtain the actual force resisted by the specimen. Electrical strain gauges were bonded on the surface of the steel reinforcement bars of the specimen and, later, also on the CFRP confinement jacket. Lateral displacements of the specimen were measured using LVDT’s in several points along the height. Special software designed for data acquisition and for the hydraulic actuator control has been used, running in LABVIEW<sup>9</sup> environment. During testing, the axial load was kept constant by the hydraulic system, whereas the lateral force can vary cyclically under lateral displacement control conditions.

## 2. CYCLIC TEST

For all the column specimens, three repetitive cycles were applied for several peak drift ratios,  $\Delta/L$ , where  $\Delta$  is the lateral displacement and  $L$  is the clear length of the column model measured between the bottom and the application point of the lateral force. Thus, the following drift ratios were considered: 0.19%, 0.31%, 0.63%,

<sup>9</sup> LABVIEW is a patented software by National Instruments.

0.25%, 0.75%, 0.94%, 0.47%, 1.25%, 1.56%, 1.88%, 2.19%, 2.50%, 2.81%, 3.13%, 3.75%, 4.38%, 5.00% and 5.63%. However, the experimental test of the column PA1-N2 was stopped after the 60mm cycle, due to an unexpected rotation of the column on the transversal direction of analysis – perpendicular direction of the actuator which coincides with the less stiff column direction.

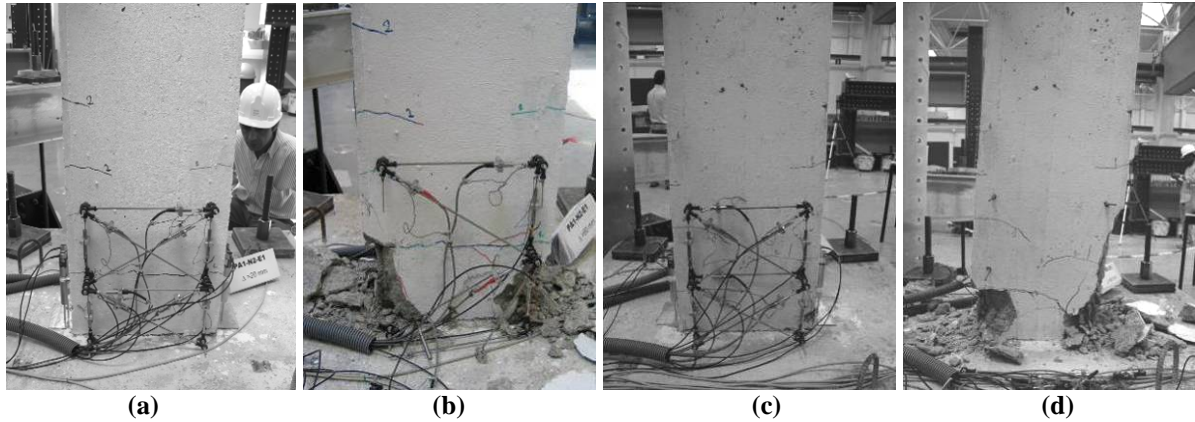


**Figure 2: Damage patterns in the column PA1-N2 (a and b) and PA1-N3 (c and d).**

Figs. 2 and 3 shows the damage reached during the test for columns PA1-N2 (2a and 2b), PA1-N3 (2c and 2d) and PA1-N6 (3a). For both columns, before 20 mm, little damage was achieved at the first cycles, where only small cracks are visible (Fig. 2a and 2c), and severe damage was found at the end of the tests, Fig. 2b and 2d, exhibiting buckling and rupture of the four corner reinforcement bars as well as significant degradation of the concrete.

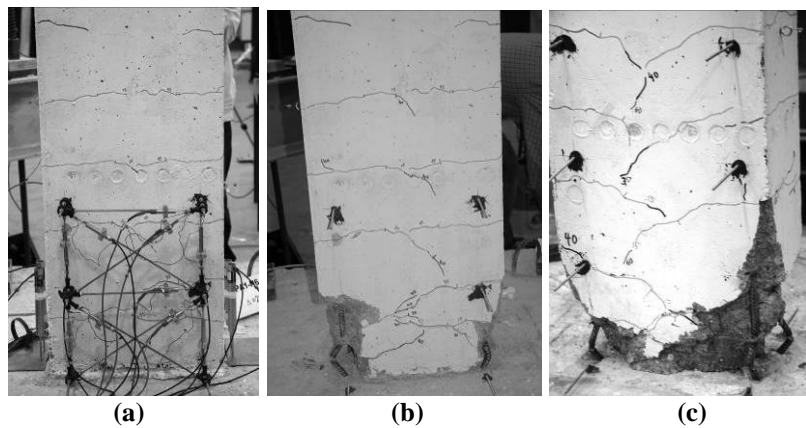


**Figure 3: Damage patterns in the column PA1-N6.**

The setup structure, more precisely the vertical steel frame, supporting the vertical actuator and the corresponding steel plate system for the axial force transmission, as well as one load cell connected to the referred steel plate with a stiff bar, were carefully observed and instrumented to understand the stiffness of each element and the corresponding distribution of forces and displacements. This procedure plays an important role due to the friction force developed in the interface of the steel plates of the axial force transmission and to the top rotation of the column that leads to the same rotation on the steel plate of the axial load system, thus producing a horizontal component of the axial force. During the tests, the load cell measurements give the force transmitted to steel plate (due to the referred effects) that should be subtracted from the horizontal actuator force to yield the force actually applied in the column.

In case of specimen PA1-N2, the buckling of longitudinal reinforcement was observed at the displacement of +50 mm, while for the opposite direction it was only observed at -60 mm. This fact justifies the asymmetric behaviour seen in Fig. 4a; it is evident the strengthening degradation for displacement larger than 60 mm at the negative direction. Meanwhile, the specimen PA1-N3 showed a good symmetry with the buckling of the longitudinal bars starting at displacement of 50 mm.

In Fig. 4a the comparison between the experimental cyclic results of the two referred columns is presented. As can be seen the results are quite close for the maximum forces achieved and globally for all the cyclic behaviour. As seen during the tests and also after analysing the results, the buckling of the longitudinal reinforcement

between the critical section (at the column base) and the first hoop affects drastically the column behaviour, which leads the quickly degradation on strengthening.

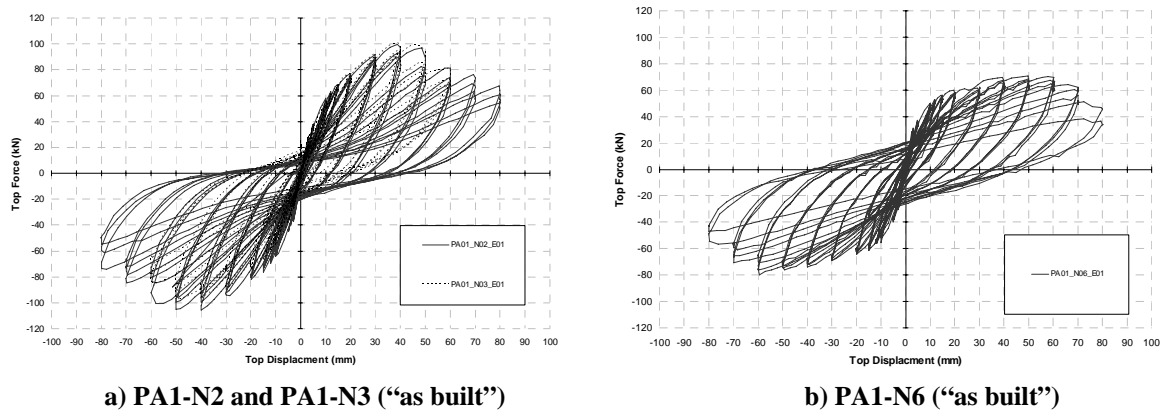


**Figure 4: Experimental cyclic results of columns**

During the tests performed to date except PA1-N6, an undesired problem occurred with the hydraulic system used to apply the axial load: the pressure that should remain constant has in fact increased. Actually, the hydraulic system was designed to keep constant the oil pressure, in order to maintain constant the axial force, but a deficient performance of the circuit has blocked the return of the oil from the vertical actuator; therefore, the axial load increased during the cyclic displacement history, because the axial actuator was forced to remain in the same position when the top-end pier section was rotating and displacing.

A preliminary test to calibrate all the setup was carried out, by using a steel column hinged at the bottom, instead of the R/C specimen, and is better described in a paper presented in this conference by the same authors (Delgado, et. al 2006). The main purpose was therefore to accurately measure all the forces involved on the vertical reaction frame.

### 3. RETROFIT

After the cyclic test of the “as built” specimens took place up to failure, they were repaired and retrofitted with three different techniques: CFRP jacket; steel plates; and steel plates connected by equal legs angles steel profiles. Before performing the retrofit all specimens were prepared according to the following steps:

- 1) Delimitation of the repairing area (the critical section at the plastic hinge region taking out all the damaged concrete - from the footing up to 30 cm above the column height);
- 2) Removal and cleaning of the damaged concrete (Fig. 5a);
- 3) Alignment and replacement of the longitudinal reinforcement bars (it was needed to cut 2 to 4 cm of the corner bars that had buckled and failed in order to ensure the alignment. The additional bars were bonded in the footing within 20 to 25 cm depth with epoxy resin and lap spliced along 20 cm);
- 4) Application of formwork and new concrete (Microbeton, a pre-mixed micro concrete, modified with special additives to reduce shrinkage in the plastic and hydraulic phase);

To have an idea of the damaged column, the following pictures illustrate the column during repairing and after retrofitted with the three techniques used in this project (Fig. 5).

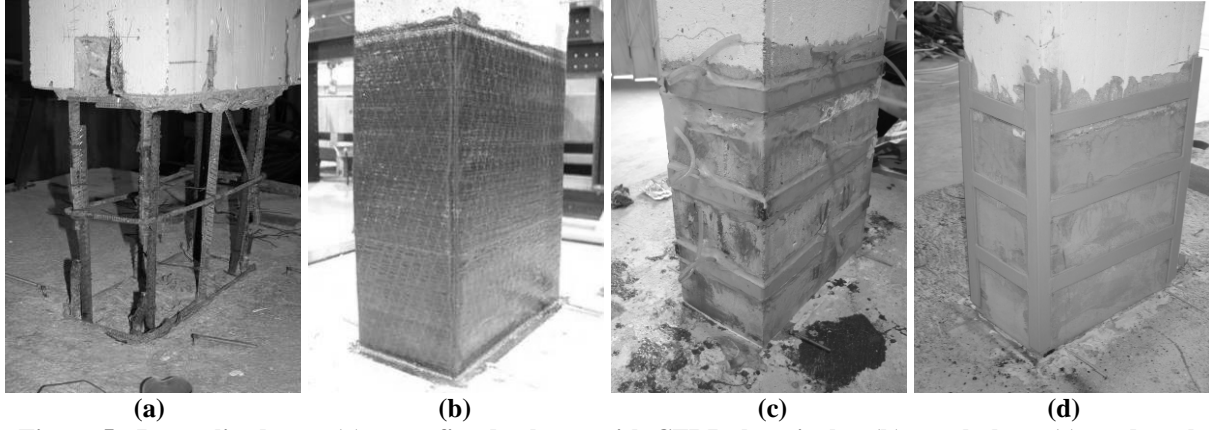


**Figure 5: Lap spliced zone (a); retrofitted column with CFRP sheet jacket (b); steel plates (c); and steel plates connected by equal leg angle steel profiles (d).**

### 3.1. CFRP Sheets Retrofit

In order to design the retrofit jackets (Fig. 5b), the authors used the Priestley et al. approach to calculate the thickness of the jacket for rectangular column to achieve a target displacement of  $\Delta = 50$  mm at the point of horizontal force application, i.e. 1600 mm above the footing, keeping the initial conditions (without upgrade of ductility and strength).

Inelastic deformation capacity of flexural plastic hinge regions can be increased by recourse to confinement of the column concrete with an advanced composite fiber jacketing system. The required volumetric ratio of confinement,  $\rho_s$ , is given by  $\rho_s = 2 t_j (b+h) / (bh)$ . On the other hand, the composite-material jackets indicate greater efficiency and are given by the following equation taken from [Priestley et al., 1996]:

$$\varepsilon_{cu} = 0.004 + \frac{1.25 \rho_s f_{ju} \varepsilon_{ju}}{f'_{cc}} \quad (1)$$

For rectangular columns the required jacket thickness can be solved from equation 1 as

$$t_j = \frac{0.4(\varepsilon_{cu} - 0.004) f'_{cc}}{f_{ju} \varepsilon_{ju}} \left[ \frac{bh}{b+h} \right] \quad (2)$$

where,  $b$  and  $h$  are the width and depth of the rectangular section and  $\varepsilon_{ju}, f_{ju}$  refer to the ultimate tensile strain and strength, respectively, of the retrofit jacket material. The compression strength of the confined concrete,  $f'_{cc}$ , is calculated from the Mander et al. (1988) equation:

$$\frac{f'_{cc}}{f'_{co}} = 2.254 \sqrt{1 + 7.94 \frac{f_l}{f'_{co}}} - 2 \frac{f_l}{f'_{co}} - 1.254 \quad (3)$$

Note that in equation 3 the lateral pressure ( $f_l$ ) can be determined for each direction  $x$  and  $y$  by

$$\begin{aligned} f_{lx} &= K_e \rho_x f_{yh} \\ f_{ly} &= K_e \rho_y f_{yh} \end{aligned} \quad (4)$$

where  $K_e$  is the sharp factor (0.75 for rectangular sections);  $\rho_x, \rho_y$  stand for the transversal reinforcement ratio in direction  $x$  and  $y$ , respectively;  $f_{yh}$  is the yield strength of transverse reinforcement and  $f'_{co}$  refers to the maximum feasible compressive strength of unconfined concrete.

Meanwhile, the ultimate compression strain,  $\varepsilon_{cu}$ , in concrete can be calculated according to the steps summarized below [Priestley et al., 1996]:

1. Based on plastic collapse analysis, the required plastic rotation  $\theta_p$  of the plastic hinge is established.
2. The plastic curvature is found from the expression  $\Phi_p = \theta_p / L_p$  where the plastic hinge length  $L_p$  is estimated by  $L_p = g + 0.044 f_y d_{bl}$ , where  $g$  is the gap between the jacket and the supporting member (in this case, the footing) (normally taken as 51 mm, but in our case it was zero).
3. The maximum required curvature is  $\Phi_m = \Phi_y + \Phi_p$ , where the equivalent bilinear yield curvature ( $\Phi_y$ ) may be found from moment-curvature analysis.
4. The maximum required compression strain is given by  $\varepsilon_{cm} = \Phi_m c$ , where  $c$  is the neutral-axis depth (from moment-curvature analysis or flexural strength calculations).

The adapted carbon fibre jacket properties are: Elastic modulus ( $E_f$ ) = 240,000 MPa; Ultimate strain ( $\epsilon_{fu}$ ) = 0.0155; ultimate strength ( $f_{fu}$ ) = 3800 MPa; layer thickness ( $t_{f1}$ ) = 0.117 mm. Using the above equations 1 - 4 and taking into account the mentioned properties of the carbon fibre sheet, and also the compressive strength of 68.5 MPa for the concrete (Microbeton) in the repaired region, three layers were used to retrofit the first specimen, PA1-N1 ( $t_f$ =0.351 mm).

For comparison purposes, it was also interesting to retrofit an undamaged specimen, PA1-N4, with CFRP jacket. This specimen was retrofitted with the same number of layers (three) and following the same order as PA1-N1, with the same conditions of surface preparation and the same operators.

The cyclic test of this specimen showed good performance and it went up to the limit of the setup, without significant degradation of the specimen.

### 3.2. Steel Plate Retrofit

In order to achieve the same target displacement mentioned at the first technique (CFRP sheets retrofit), the specimen PA1-N2 was retrofitted with steel plates (Fig. 5c) after a previous cyclic test. The steel plates were designed following the Priestley approach for steel jacket [Priestley et al., 1996]; after the thickness of the steel jacket is calculated, it is multiplied by the length of the jacket yielding the total area per face. To reduce this jacket into plates, a fixed width was chosen leading then a new jacket thickness. It can be summarized in the following steps:

1. Using the Priestley approach, the thickness of the steel jacket is obtained by equation 2;
2. For easy comparison, the steel jacket will have the same height as the CFRP jacket along the column, i.e., 500 mm.
3. Thus, a total area of the steel jacket per face is obtained; this area was then divided by the number of steel strip plates (three plates were adopted);
4. Finally, fixing the plate width (30 mm in the present case), a new thickness of the steel plates was obtained.

The steel plates were L-shape folded and welded in situ in two corners to complete the collar. The plates were placed in three previously defined levels at increasing distances from the footing (125 mm, 275 mm and 425 mm). Voids between the plates and the concrete were then filled with injection of two component epoxy resin.

Since the concrete compressive strength in the repaired region is  $f'_{co}$  = 68.5 MPa, the compressive strength of the confined concrete becomes  $f'_{cc}$  = 77 MPa. The ultimate steel strength is 235 MPa at a ultimate strain of 0.15. Taking into account the above material properties, a steel jacket thickness  $t_j$  = 0.536 mm was obtained, which led to a total area of 268 mm<sup>2</sup> per face; this total area per face was then divided by three to obtain the steel plate areas (89.333 mm<sup>2</sup>). With the fixed width, a new thickness was achieved, about 3 mm.

### 3.3. Retrofit by steel Plates connected by equal leg angle profiles

After the total removal of the damaged concrete, as a consequence of cyclic tests of the specimen PA1-N3, it was repaired with microbeton, as described in the specimen PA1-N1. The surfaces areas were prepared to receive the same steel plates as obtained for the specimen PA1-N2 retrofit but with additional longitudinal steel angle profiles in the corners of the column section (Fig. 5d – PA1-N3-R1), with the same thickness, and the three plates welded in both sides of the L-shaped longitudinal steel angle and other two L-shaped to complete the four corners. A gap of 30 mm between the L-shaped longitudinal steel angles and the footing were left in order to avoid an increase in the strengthening at the critical section, as the main objective of this retrofit is also to maintain the same ductility. The injection of a material based on epoxy resin with two components was undertaken after the welding works in situ were concluded. This type of retrofit solution was used with a foundation connection, that obliged the vertical profiles behave like an increase of the longitudinal reinforcement (PA1-N3-R1).

## 4. CYCLIC TEST OF THE RETROFITTED SPECIMENS

The retrofitted column PA1-N1 was tested following the same cyclic displacement history of the “as built”. As can be seen in the Fig. 6, the retrofitted specimen showed a good behaviour in comparison with the “as built”, exhibiting flexural cracking along the CFRP jacket (Fig. 6a and 6b), very distributed and reaching the region above the jacket for both lateral displacement direction. The CFRP jacket failure took place at 65 mm (drift = 4.0%) lateral displacement preceded by the noise of the fibre rupture (Fig. 14b). At the failure stage the experimental strain on the concrete, obtained from the LVDT's measurements, was around 6.3‰ whereas the numerical prediction was pointing to 6.8‰, using the equations 1 – 4. The results suited satisfactory, confirming the equations proposed by [Priestley et al., 1996].



During this test some unexpected displacements occurred on the steel portal that support the vertical hydraulic jack, more precisely a horizontal displacement on one of its foots fixed to the strong floor. This incident affected the obtained results on the load cell connected to the upper steel plate. Thus, higher forces for the north direction of the actuator displacements and lower forces in the opposite direction were measured, due to the reduced stiffness of the steel portal on the north direction. Therefore, these experimental results could have increased forces throughout the south displacement direction, negative displacements in Fig. 7, where the results for the original and retrofitted column are compared. As expected this retrofit solution applied to an “as build” specimen shows an excellent behaviour in both ductility and strength capacity as can be seen in Figs. 6c, 6d and 7b.

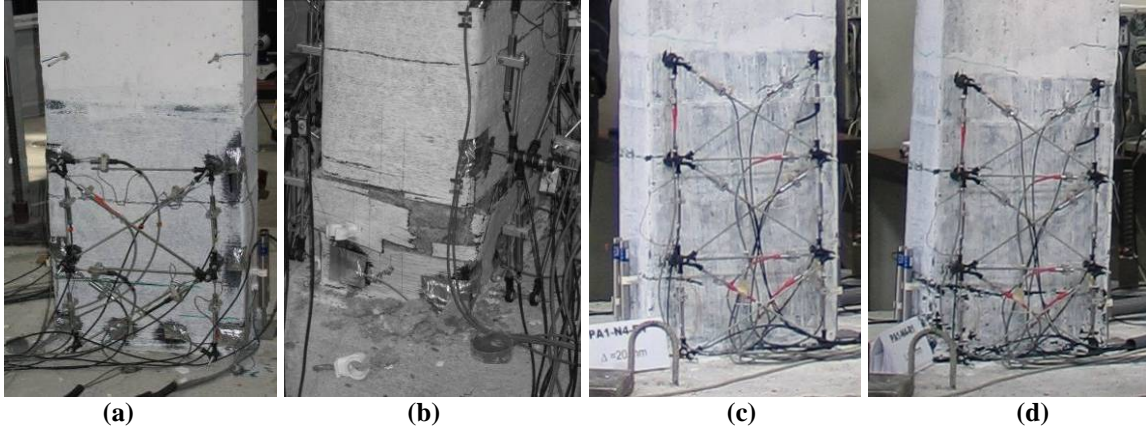
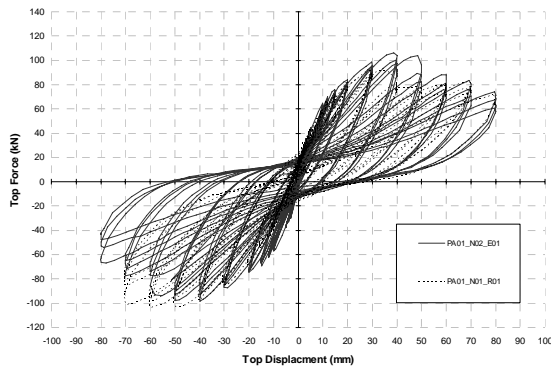
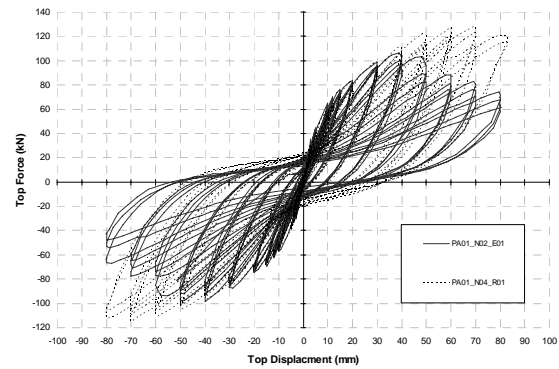


**Figure 6: Damage on the CFRP retrofitted specimen: flexural cracking (a and c) and failure (b and d).**



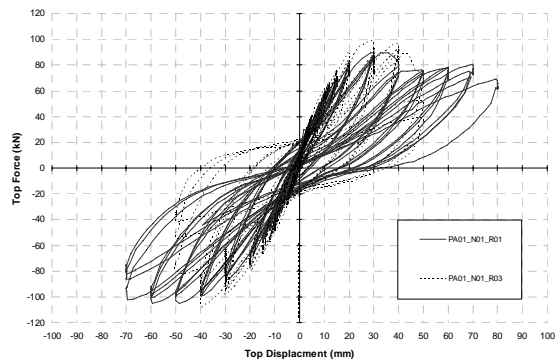
**a) PA1-N2 “as built” and PA1-N1-R1**



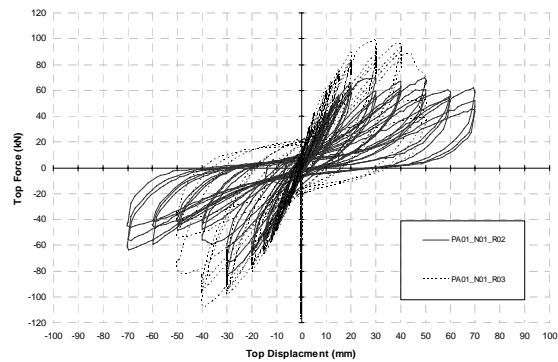
**b) PA1-N2 “as built” and PA1-N4-R1**

**Figure 7: Comparison between CFRP retrofit solutions.**

In order to establish the benefits of using the CFRP retrofit solutions, two tests were performed only repairing the damage area but without applying the CFRP sheets and using two different ways of connect the longitudinal reinforcement bars to the base: with an overlapping of about 20cm (PA1-N1-R2); and, the same overlapping with weld connection (PA1-N1-R3).



**a) PA1-N1-R1 and PA1-N1-R3**



**b) PA1-N1-R2 and PA1-N1-R3**

**Figure 8: Comparison between CFRP retrofit solution with two solutions of connect the reinforcement longitudinal bars.**

In the first case, (Fig. 8a) overlapping with weld connection, the behaviour of the rebuild specimen was quite similar to the CFRP retrofit solution, leading to conclude that the CFRP sheets confinement are enough to make efficient the strength transmission through the longitudinal reinforcement and therefore avoiding the lap slide. Comparing the two ways of connect the longitudinal reinforcement bars (Fig. 8b), the weld is efficient at the first cycles but due to the fragility on the repair and original concrete zone the damage is highly concentrated and leads to a quick decrease of flexural capacity.

The test of the retrofit solution applied on PA1-N2 column – steel plates - is illustrated in the Fig. 9. Very small and distributed flexural cracking was achieved during the first cycles, about 20 mm (Fig. 9a). For the maximum displacements cycles (Fig.9b) the retrofitted specimen showed a quite good behaviour in comparison with the “as built”, with only local damage below the lower steel plate.

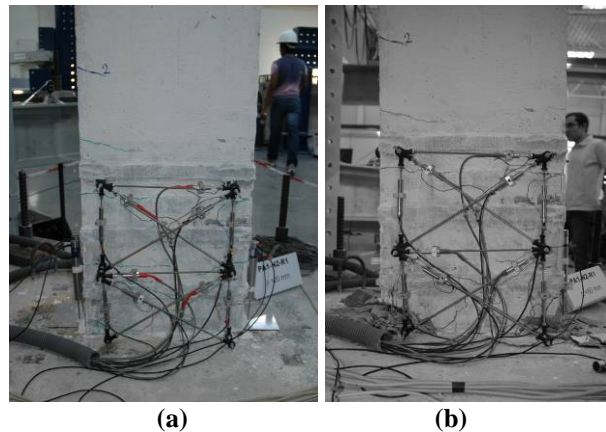


**Figure 9: Damage on the retrofitted specimen PA1-N2: flexural cracking (a) and failure (b).**

Before the buckling of longitudinal reinforcement the “as built” and retrofitted specimens had similar behaviour, as a consequence of the concrete confinement effectiveness, as can be seen in Fig. 10. The retrofit applied to specimen PA1-N2, and experimentally tested in the laboratory, has shown a satisfactory solution to the buckling problem since it brought a significant strength increase in the final cycles of displacement, doubling the residual strength of the “as built” specimen.

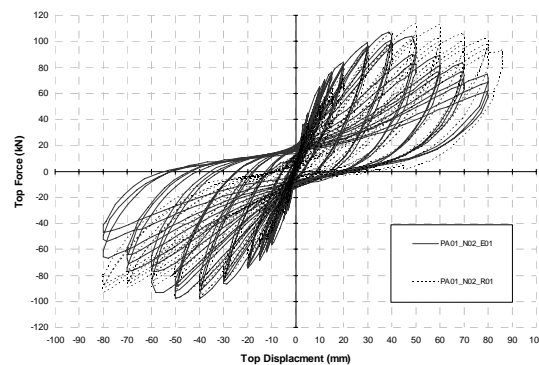


**Figure 10: Experimental cycle results for the original and retrofitted PA1-N2 column.**

In Fig. 11(a and b) the experimental test carried out on column PA1-N3-R1 retrofitted with steel plates connected by equal leg angle steel profiles is illustrated. Again very small and distributed flexural cracking was achieved until the 20 mm cycles (Fig. 11a). For the maximum displacement cycles (Fig. 11b) the retrofitted specimen showed a quite good behaviour in comparison with the “as built”, with very small and local damage below the lower steel plate, more precisely at the column base crack. Fig. 12a shows the same conclusions taken from Fig. 10 which are applied to this case of retrofit. In Fig. 11(c and d) is presented the flexural cracking and failure of the retrofit steel plates connected to the foundation. This type retrofit showed a lack of efficiency because the reinforcement was not prepared to resist shear strength that produce the earlier collapse of the connection between the corner and side retrofit of the steel plates. This fact can be seen in Fig. 12b, where in the first cycles a slight increase of flexural capacity is achieved but a significant reduction of strength is obtain for cycles above 30mm top displacement.



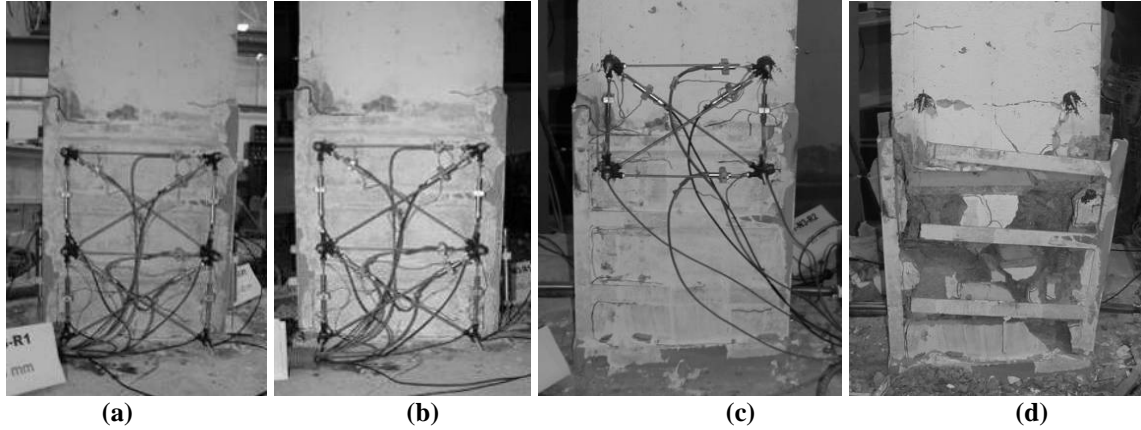
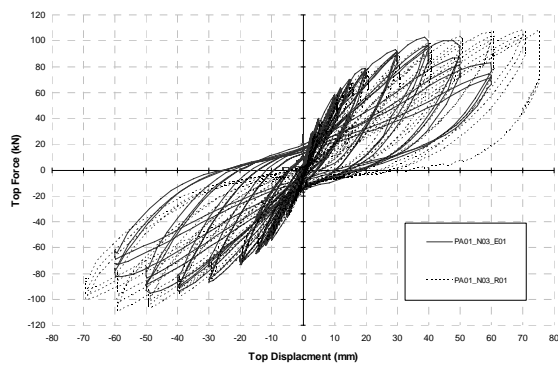
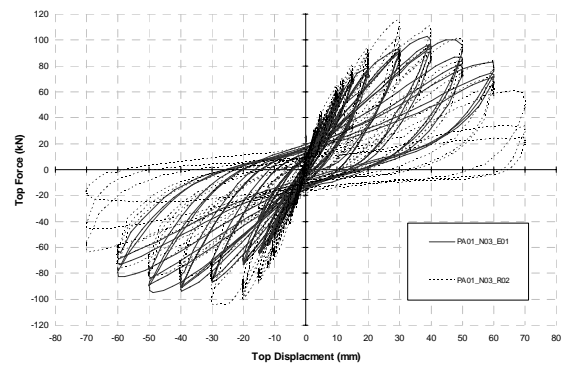


**Figure 11: Damage on the retrofitted specimen PA1-N3: flexural cracking (a and c) and failure (b and d).**



**a) PA1-N3 “as built” and PA1-N3-R1**



**b) PA1-N3 “as built” and PA1-N3-R2**

**Figure 12: Comparison between steel plates connected by profiles retrofit solutions.**

The results obtained from the two retrofit techniques with steel are almost similar, although the specimen PA1-N3 showed an improved behaviour in terms of strength degradation (Fig.12a). This small improvement can be justified by the steel angles profiles added to the strips at the corners of this specimen; even without being connected to the footing, the steel angles profiles avoided the cover concrete spalling, particularly close to the critical zone, which improves the strength capacity of the compressive zone. On the other hand, a possible comparison between the steel retrofit with the CFRP retrofit in the first specimen PA1-N1, could lead to a similar result of the two other retrofit techniques compared above. This hypothesis must be confirmed through a new test with an improved connection of the vertical portal frame to the strong floor, in order to avoid the slipping observed in the first experimental test.

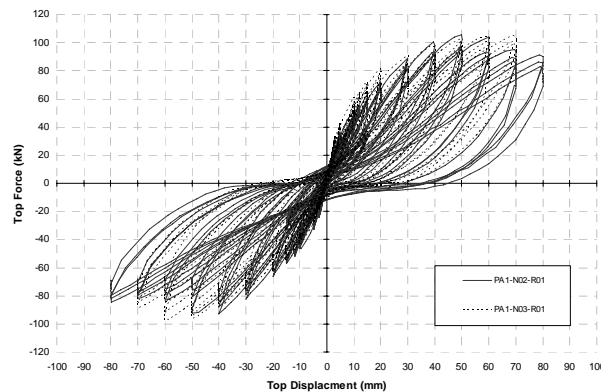


**Figure 13: Comparison between the two steel retrofit techniques.**

## 5. CONCLUSIONS

The setup used within this framework shows a very good performance to carry out bending tests with axial load. The slide device, a steel plate system for the axial force transmission that allows the top displacements of the column, performed satisfactorily and showed low values of friction forces.

Since the retrofit objective was basically the reestablishment of the original conditions, no strength and ductility increase was observed, as expected. Furthermore, the experimental strain at the failure stage was close to the numerical prediction strain obtained using Priestley approach. From the observation of the experimental tests and their results it is possible to conclude that restraining the longitudinal reinforcement buckling by transversal retrofit have significant benefit in behaviour and particularly leading to lower strength degradation.

The CFRP retrofit solution when applied for repair the column behave quite close to overlapping with weld connection technique (without CFRP sheets confinement), leading to conclude that the lap slide is satisfactorily avoid, due to an efficient strength transmission through the longitudinal reinforcement. As expected this retrofit solution applied to an “as build” specimen shows an excellent behaviour in both ductility and strength capacity.

The two steel retrofit techniques showed a satisfactory solution to the buckling problem and brought a significant strength increase in the final cycles of displacement, doubling the residual strength of the “as built” specimen. However, when connected to the foundation this retrofit could decrease significantly the column capacity for higher displacements.

The comparison between the two retrofit techniques with steel showed an almost similar behaviour with a very small improvement of strength degradation on steel plates connected by equal leg angle profiles, cause by better cover concrete spalling which improves the strength capacity of the compressive zone.

Any of the proposed retrofit led to strong concentration of deformation and the concrete degradation at the critical section (base) of the specimens reducing significantly the plastic hinge length.

## 6. ACKNOWLEDGEMENTS

The authors acknowledges also João da Silva Santos, Lda company, for the construction of the columns tested and S.T.A.P.- Reparação, Consolidação e Modificação de Estruturas, S. A. company for the repair and retrofit works. Final acknowledges to the laboratory staff, Eng.<sup>a</sup> Daniela Glória and Mr. Valdemar Luís, for all the careful on the test preparation.

## 7. REFERENCES

- Delgado, P., Rocha, P., Rodrigues, V., Santos, M., Arêde, A., Vila Pouca, N., Costa, A. and Delgado, R. (2006), Experimental Cyclic Tests and Retrofit of RC Hollow Piers, *1st European Conference on Earthquake Engineering and Seismology*, September 3-8, Geneva, Switzerland: *Paper N. 1205*.
- Delgado, P., Costa, A., Delgado, R. (2004), Different Strategies for Seismic Assessment of Bridges – Comparative studies, *Proceedings of the 13th World Conference on Earthquake Engineering*, August 1-6, Vancouver, Canada: *Paper N. 1609*.
- Delgado, P., Costa, A., Delgado, R. (2005), Safety Assessment of Bridges Subjected to Earthquake Loading. (Submitted).
- Mander, J. B., Priestley, M. J. N. and Park, R. (1988), Theoretical Stress-Strain Model for Confined Concrete, *Journal of the Structural Division*, ASCE, Vol. 114, N° 8, pp 1804-1826.
- Pinho, R. (2000), Selective retrofitting of RC structures in seismic areas. London: PhD Thesis, Imperial College of Science and Technology.
- Priestley, M. J. N., Seible, F., Calvi, G. M. (1996), Seismic Design and Retrofit of Bridges, *John Wiley & Sons*, New York.
- Rocha, P., Delgado, P., Costa, A., Delgado, R. (2004), Seismic retrofit of RC frames. *Computers & Structures*, 82, pp 1523-1534. Elsevier.
- Vaz, C. T. (1992), Comportamento Sísmico de Pontes com Pilares de Betão Armado. PhD Thesis. FEUP/LNEC.
- Varum, H. (2003), Seismic assessment, strengthening and repair of existing buildings, PhD Thesis.